Electrochimica Acta 94 (2013) 124–133

Contents lists available at SciVerse ScienceDirect

Electrochimica Acta

journal homepage: www.elsevier.com/locate/electacta

Effect of chitosan on distearoylphosphatidylglycerol films at air/water and liquid/liquid interfaces

Candelaria I. Cámara[a,1], Mónica V. Colqui Quiroga[a,1], Natalia Wilke[b,2], Alvaro Jimenez-Kairuz[c,3], Lidia M. Yudi[a,*]

[a] Instituto de Investigaciones en Fisicoquímica de Córdoba (INFIQC-CONICET), Departamento de Fisicoquímica, Facultad de Ciencias Químicas, Universidad Nacional de Córdoba, Ala 1, Pabellón Argentina, Ciudad Universitaria, 5000 Córdoba, Argentina
[b] Centro de Investigaciones en Química Biológica de Córdoba (CIQUIBIC-CONICET), Departamento de Química-Biológica, Facultad de Ciencias Químicas, Universidad Nacional de Córdoba, Ala 1, Pabellón Argentina, Ciudad Universitaria, 5000 Córdoba, Argentina
[c] Departamento de Farmacia, Facultad de Ciencias Químicas, Universidad Nacional de Córdoba, Haya de la Torre y medina Allende, Ciudad Universitaria, 5000 Córdoba, Argentina

ARTICLE INFO

Article history:
Received 18 November 2012
Received in revised form 20 January 2013
Accepted 25 January 2013
Available online 4 February 2013

Keywords:
Chitosan
Phospholipids monolayers
Liquid/liquid interfaces
Air/water interfaces
Cyclic voltammmetry
Langmuir isotherms

ABSTRACT

The effect of chitosan on distearoylphosphatidylglycerol (DSPG) films was analyzed by cyclic voltammetry, surface pressure-area and surface potential-area isotherm and Brewster Angle Microscopy. Experiments of cyclic voltammetry at a liquid/liquid interface demonstrated a blocking effect of DSPG to tetraethylammonium (TEA^+) cation transfer from the aqueous to the organic phase. This effect was reversed by the presence of chitosan, which modifies the film structure. Special emphasis was placed on the nature of the supporting aqueous electrolyte (LiCl or $CaCl_2$). In the presence of LiCl the permeability of the film increases when chitosan is present in the aqueous phase, minimizing the blocking effect of the film on TEA^+ transfer probably due to the presence of bare zones at the interface. Oppositely, in presence of Ca^{2+}, the enhancement of permeability was not observed, probably due to the impediment of chitosan to penetrate into the very tightly compacted film of DSPG. Electrochemical experiments were completed with viscosity measurements to explain the variation of diffusion coefficients for TEA^+. Isotherms of compression for DSPG monolayers modified with chitosan, demonstrate that this polymer produces an expansion of the DSPG film and modifies the compression factor, for both electrolytes studied. Images of Brewster angle microscopy evidence an increase in the optical thickness of the DSPG films in presence of chitosan indicating that the polymer interacts with DSPG molecules at low and high molecular areas.

1. Introduction

Chitin is a homopolymer of β (1–4)-linked N-acetyl-D-glucosamine and the second abundant natural polymer after cellulose. It is found in the exoskeleton of many invertebrates and in the cell walls of most fungi [1]. Chitosan (Scheme 1), is a natural polyaminosaccharide [2,3] obtained by N-deacetylation of chitin. It contains multiple amino groups, which give a skeleton with high positive charge when is dissolved in acid medium ($pK_a = 6.9$). The growing interest in the study of the chitosan chemistry is based on its properties of biocompatibility, biodegradability and low cytotoxity [3,4]. These features become this polymer in an excellent candidate for medical applications. As a consequence of its important properties, chitosan has been used for a large number of applications including: chelating of heavy metal ions [5–7], fat reducer agent [8], drugs [9,10] and gene delivery systems [11], bactericide agent [12] and blood coagulation [13] among others.

Recent studies demonstrate that chitosan can interact with liposomes [14], proteins [15–17], lipids [18,19] and biomembranes [20–24], and emphasize the importance of understanding the nature of such interactions because most of the uses of chitosan involve the contact with cell membranes.

Parra-Barraza et al. investigated the influence of chitosan in the properties of cholesterol and stearic acid monolayers, demonstrating that this polyelectrolyte alters the rigidity of the monolayers [25]. On the other hand, data on compression isotherms of Langmuir monolayers and transfer to solid supports as Langmuir–Blodgett films and infrared microscopy [26] demonstrated that chitosan interacts with dimyristoyl phophatidic acid (DMPA) monolayers, causing expansion and decreasing the monolayer elasticity. In that work, the authors propose a model in which chitosan interacts with DMPA film via dipole and electrostatic interactions. Additionally, recent studies reported by Silva et al.

* Corresponding author. Tel.: +54 0351 4334169/80; fax: +54 0351 4334188.
E-mail addresses: mjudi@fcq.unc.edu.ar, mabelyudi@gmail.com (L.M. Yudi).
[1] Tel: +54 0351 4334169/80; fax: +54 0351 4334188.
[2] Tel.: +54 0351 4334171/68.
[3] Tel.: +54 0351 4334163/27.

0013-4686/$ – see front matter © 2013 Elsevier Ltd. All rights reserved.
http://dx.doi.org/10.1016/j.electacta.2013.01.137

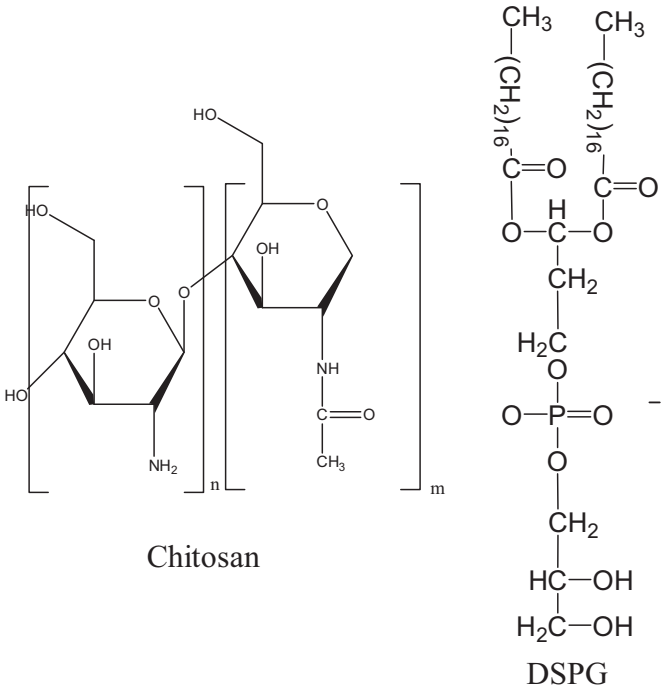

Scheme 1. Structures of chitosan and DSPG.

demonstrate that chitosan forms a complex with mucin in DMPA monolayers, based on electrostatic interaction [17].

Electrochemical measurements applied to liquid–liquid interfaces modified by different films have been carried out in the last decades with the aim of developing new biomimetic membranes models. In this sense, the adsorption of lipid monolayer [27,28], proteins [29,30] or polyelectrolyte [31] has been studied and the properties of these films have been characterized by cyclic voltammetry, electrochemical impedance spectroscopy, and surface tension measurements. One aspect of special interest has been the study of the interaction or the complex formation between phospholipid monolayers and alkaline or alkaline earth cations [32], or peptides [33], as well as between polyelectrolytes with different ions [34,35] and DNA [36]. All references listed above demonstrate that electrochemical techniques applied at the interface between two immiscible electrolyte solutions (ITIES) are ideal to follow dynamic changes in the lipid layer compactness and interfacial interactions at a hydrophobic/hydrophilic boundary.

In previous papers we have studied the incorporation of anxiolytics drugs into the phospholipid monolayers adsorbed at liquid/liquid interfaces [37–41]. The results obtained contribute to the knowledge of the non-specific interaction between these drugs and biological membranes components, which is particularly important because their accumulation in biomembranes alters the structural properties leading to collateral effects. The combination of surface pressure - molecular area measurements and electrochemical experiments employing a test cation such as tetraethyl ammonium (TEA^+) allowed us to evaluate the permeability and the compactness of the monolayer. In the present paper we studied the effect of chitosan on distearoylphosphatidylglycerol (DSPG) films formed at water/1,2-dichloroethane or at air/water interfaces, employing different experimental setups and techniques such as viscosity measurements, surface pressure–molecular area and surface potential–molecular area isotherms, Brewster angle microscopy and cyclic voltammetry. Special emphasis is placed in the composition of the aqueous phase which contained LiCl or $CaCl_2$ as electrolytes that, in turn, modified the effect of chitosan on DSPG films.

2. Experimental

2.1. Materials and electrochemical cell

Cyclic voltammetry (CV), performed in a four-electrode system using a conventional glass cell of 0.16 cm^2 interfacial area, was conducted to characterize the film. Two platinum wires were used as counter electrodes and the reference electrodes were Ag/AgCl. The reference electrode in contact with the organic solution was immersed in an aqueous solution of 1.0×10^{-2} M tetraphenylarsonium chloride (TPAsCl, Aldrich). Potential values (ΔE) reported in this work are those which include $\Delta\phi^0_{tr,TPAs^+} = 0.364$ V for the transfer of the reference ion $TPAs^+$.

The base electrolyte solution were 1.0×10^{-2} M MCl_z ($M^{z+} = Ca^{2+}$, Li^+) (p.a. grade) in ultra pure water and 1.0×10^{-2} M tetraphenyl arsonium dicarbollyl cobaltate (TPAsDCC) in 1,2-dichloroethane (DCE, Dorwill p.a.). TPAsDCC was prepared by metathesis of TPAsCl and sodium dicarbollyl cobaltate (Aldrich p.a.). The pH of the aqueous solution was 3.00, adjusted with 2.00% (v/v) acetic acid glacial (Baker Analyzed). In all experiments 1.00 mL of organic and 4.00 mL of aqueous phase were used to fill the cell. In other set of experiments, the organic phase was gelled. For this purpose, 10.00% (w/v) HMW-PVC and 30 μL of Dioctyl Sebacate (Química Olivos S.A. C.I) were added to 1.00 mL of organic phase and heated at 75 °C for 3 min.

The electrochemical cell used was as follows:

		TPAsCl	TPAsDCC	MCl_n		
Ag	AgCl	$1x10^{-2}$ M	$1x10^{-2}$ M	$1x10^{-2}$M	AgCl	Ag
		(w′)	(o)	(w)		

Pure Chitosan (Sigma–Aldrich, MW: 50–190 KDa, >75% deacetylated) was added to the aqueous phase (w) in a concentration range from 0 to 1.00% (w/v).

Distearoylphosphatidylglycerol (DSPG) was of analytical grade (Sigma–Aldrich). A solution containing 0.80 mg/mL of DSPG in 1:2 methanol:chloroform was prepared. In order to form the lipid film, 50 μL of DSPG solution were injected, using a Hamilton microsyringe, at the liquid/liquid interface after both phases were put in contact in the electrochemical cell. A time equal to 60 min after the injection of the lipid solution was required to obtain reproducible voltammetric response, indicating that a stable lipid film had been formed. As a consequence, all experiments were performed after this equilibration time at room temperature equal to 25 ± 1 °C. Temperature was controlled with a temperature/humidity monitor.

It is important to remark that at pH 3.00 chitosan is positively charged while the polar head groups of DSPG molecules at the interface are partially ionized with negative charge.

2.2. Cyclic voltammetry (CV) experiments

Voltammograms were carried out using an aqueous solution of 5×10^{-4} M tetraethylammonium chloride (TEACl, Sigma). The cation TEA^+ was employed as a probe ion, since it transfers from the aqueous to the organic phase according to a direct reversible diffusion controlled mechanism [37]. The comparison between the voltammetric profiles for TEA^+ before and after injection of DSPG, in the absence and in the presence of chistosan dissolved in the aqueous phase, allows us to evaluate the ion permeability of the monolayer.

CV experiments were performed using a four-electrode potentiostat with periodic current interruption for automatic elimination

of solution resistance. The voltage was changed from 0.200 V to 0.750 V with a potential sweep generator (L y P Electrónica, Argentina). Voltammograms were recorded employing a 10 bit computer board acquisition card connected to a personal computer. Voltammograms with typical errors of ±10% in current values were obtained.

2.3. Viscosity experiments

Viscosity measurements were performed in a rotational viscotester (Haake Viscotester VT500, Termo Scientificric, Karlsruhe, Ger.) equipped with standard sensors, MV cup and MV2 cylinder, as measuring systems. Data were collected and analyzed using the specifics software VT500, 3.01version.

The apparent viscosity (η) was calculated from the linear portion of flow curves, obtained at shear rates ranging from 10 s^{-1} to 550 s^{-1}. All measurements were carried out at 25 °C. Three replicates were tested for each sample and three measurements were performed for each replicate.

The composition of the aqueous solutions analyzed was: 1.0×10^{-2} M LiCl, 2.00% (v/v) acetic acid and chitosan in a concentration range from 0% (w/v) to 1.00% (w/v), pH 3.00. The solutions were prepared from a 2.00% (w/v) chitosan stock solution.

2.4. Langmuir monolayers

2.4.1. Surface Pressure - molecular area isotherms

Surface pressure - molecular area isotherms were recorded with a mini-trough II from KSV Instruments Ltd. (Helsinki, Finland). The surface tension was measure using the Wilhelmy plate method with a platinum plate.

The aqueous subphase, contained in a Teflon trough (364 mm × 75 mm effective film area), was 1.0×10^{-2} M MCl_z (M^{z+} = Ca^{2+}, Li^+), 2.00% (v/v) acetic acid pH 3.00 with or without chitosan at different concentrations.

To prepare DSPG monolayers at the air–water interface, 30 μL of DSPG solution in 1:2 methanol:choloform (0.40 mg/mL) was carefully spread at the surface with a Hamilton micro-syringe. Before spreading DSPG solution, the subphase surface was cleaned by sweeping it with the Teflon barriers and then, any surface contaminant was removed by suction from the interface. The cleaning of the surface was checked by recording an isotherm in absence of DSPG and verifying a surface pressure value lower than 0.20 mN/m. After spreading, the solvent was allowed to evaporate during 10 min, and then the film was compressed with two barriers, one on each side of the trough at a compression speed of 5 mm/min while the automatic measurement of the lateral surface pressure (π) was carried out.

All experiments were performed at 25 ± 1 °C using a HAAKE G. thermostat. At least two compression isotherms were registered at each condition and results with a typical area and collapse pressure errors of ±2 $Å^2$ and ±1 mN m^{-1} respectively were obtained.

The surface compression modulus κ (mN m^{-1}) was calculated from the compression isotherm as:

$$\kappa = -A \times \left(\frac{\partial \pi}{\partial A}\right)_T \quad (1)$$

where A is the molecular area per molecule and π is the surface pressure in mN m^{-1}. The uncertainty of compression modulus was ±10 mN m^{-1}.

2.4.2. Surface potential - molecular area isotherms

The Surface potential - molecular area isotherms were measured with a home-made Langmuir balance using an air-ionizing ^{241}Am plate surface electrode and an Ag/AgCl/Cl^- (3 M) reference electrode [42]. The composition of the subphases used in these compression isotherms were the same as in Section 2.4.1. To prepare DSPG film monolayer at the air–water interface volumes between 15–25 μL of DSPG in 1:2 methanol:chloroform solution (0.40 mg/mL) were carefully spread at the surface with a Hamilton micro-syringe. The experiments were performed after 10 min of the injection. The film was compressed with one barrier at a compression speed of 13 mm/min. Lateral pressure was registered simultaneously and the lateral pressure-molecular area isotherms obtained with this equipment were similar to the obtained as explained in Section 2.4.1.

2.5. Brewster angle microscopy (BAM)

The BAM experiments were carried out using an EP3 Imaging ellipsometer (Acucurion, Goettingen, Germany) with a 20x or a 10x objective. The monolayer was formed in a Langmuir film balance (KSV minitrough, KSV Instruments, Ltd., Helsinki, Finland) using the same volumes and DSPG solution than those described in Section 2.4.1. Images were registered after 10 min from the injection of DSPG solution, in simultaneous with the surface pressure-molecular area isotherm.

The optical thickness (h) was calculated from the BAM images taken after the BAM equipment was calibrated. The grey level of each section of the micrograph can then be converted to reflected light intensity (Rp), and h was calculated assuming a smooth but thin interface in which the refractive index varies along the normal to the interface on a distance h, much smaller than the incident light wavelength λ (λ = 532 nm) [42], which leads to:

$$h = \frac{\sqrt{Rp}}{\sin(2\theta_B - 90)} \left(\frac{\pi \sqrt{n_1^2 + n_2^2}(n_1^2 - n^2)(n_2^2 - n^2)}{\lambda (n_1^2 - n_2^2) n^2} \right)^{-1} \quad (2)$$

In Eq. (2) n_1, n and n_2 are the air, film and subphase refractive index, respectively and θ_B is the Brewster angle.

The refractive index used for DSPG monolayers in the absence of chitosan was 1.45, since this is the value reported for condensed films [43]. As detailed below, when chitosan was present in the subphase the DSPG film became more expanded and then, the refractive index is expected to decrease [44]. Since the refractive index at this condition was unknown, we determined the monolayer thicknesses using 1.42 (index for liquid expanded phases) and 1.45 (index for liquid condensed phases) [44] and in this way could evaluate the whole range of possible height values. The refractive index for the subphases was calculated for each experiment from the experimental Brewster angle ($n_2 = tg(\theta_B)$), using 1.00 as the refractive index of air) obtaining the following values: 1.336 for the subphase with MCl_z (M = Li^+ or Ca^{2+}) 1.00×10^{-2} M-2.00% (v/v) acetic acid in absence and 1.337 in presence of chitosan.

3. Results and discussion

3.1. Cyclic voltammetry

The effect of chitosan on DSPG monolayers was analyzed by cyclic voltammetry adding the polymer to the aqueous phase before or after the film formation at the water/1,2-dichloroethane interface. The results obtained are shown below in Sections 3.1.1 and 3.1.2. The comparison of these results allows evaluating if chitosan modifies the adsorption of DSPG molecules or the structure of the film previously adsorbed.

3.1.1. Effect of chitosan on DSPG adsorption

Fig. 1a shows the voltammetric response corresponding to TEA^+ transfer across the bare interface (solid black line) and in the presence of DSPG monolayer formed after 60 min of injecting 50 μL of

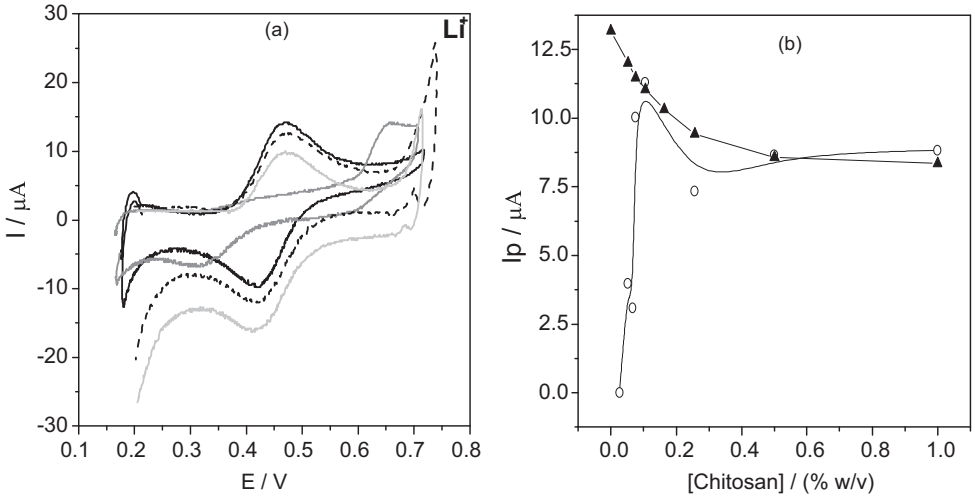

Fig. 1. (a) Cyclic voltamograms corresponding to the transfer of TEA^+ through the bare interface (▬▬) or 60 min after the injection of 50 μL of 1 mM DSPG in 1:2 methanol:chloroform solution at different concentrations of chitosan: (▬▬) 0, (---) 0.10 and (▬▬) 1.00% (w/v). (b) Dependence of Ip^+ with chitosan concentration: in presence (○) or in absence (▲) of DSPG film. Aqueous phase composition: 1×10^{-2} M LiCl, 2.00% (v/v) acetic acid, 5×10^{-4} M TEA^+, and different concentrations of chitosan, pH 3.00. Organic phase composition: 1×10^{-2} M TPhAsDCC. $\upsilon = 0.050\ V\ s^{-1}$.

1 mM DSPG solution onto aqueous phases containing LiCl as supporting electrolyte and chitosan in a concentration range from 0 to 1.00% (w/v). Solid black line corresponds to the very well known reversible diffusion controlled behavior of TEA^+ transfer process across the bare liquid–liquid interface. A forward current peak at $Ep = 0.480$ V and the corresponding backward process with a peak to peak separation $\Delta Ep = 0.060$ V can be observed. The peak current, Ip, is linear with $\upsilon^{1/2}$ over the whole range of sweep rates analyzed (not shown). If this response is compared with that obtained when the DSPG molecules are present at the interface, in absence of chitosan in the aqueous phase, an important decrease in current and a shift of 0.200 V for the positive peak potential towards more positive values and 0.120 V for the negative peak potential towards more negative values can be noticed. These changes are evidencing a blocking effect of the layer to TEA^+ transfer since it can be assumed that the transfer potential shift is due to the increase in Gibbs energy on transfer caused by the work of permeation of species across the film. However this effect decreases as chitosan concentration in aqueous phase increases, almost disappearing for a concentration equal to 1.00% (w/v) and recovering a voltammetric response close to the original one. This is a demonstration that chitosan produces disorder on the film or formation of bare zones (pores), minimizing its blocking effect on TEA^+ transfer.

Fig. 1b summarizes the effect of chitosan concentration on the DSPG monolayer structure. The variation of current values at $Ep = 0.480$ V is plotted vs chitosan concentration in absence (▲) and in presence (○) of the monolayer. The decrease in current values in absence of the film can be explained considering a decrease in diffusion coefficient of TEA^+ caused by the increase in viscosity of the aqueous phase with the chitosan concentration as it will be demonstrated below. When the monolayer is present, a marked decrease in current is observed in absence of chitosan in aqueous phase, nevertheless, for chitosan concentrations within the range 0.02–0.15% (w/v), it sharply increases from almost zero to values close to that observed in absence of the film. For chitosan concentration values higher than 0.20% (w/v) a slight decrease followed by constancy in current values are reached as a consequence of the decrease in diffusion coefficients already noted in absence of the film.

A significantly different response is obtained when LiCl is replaced by $CaCl_2$ as aqueous supporting electrolyte as can be observed in Fig. 2. It is evident from these results that the blocking effect to TEA^+ transfer caused by the monolayer is not reversed by

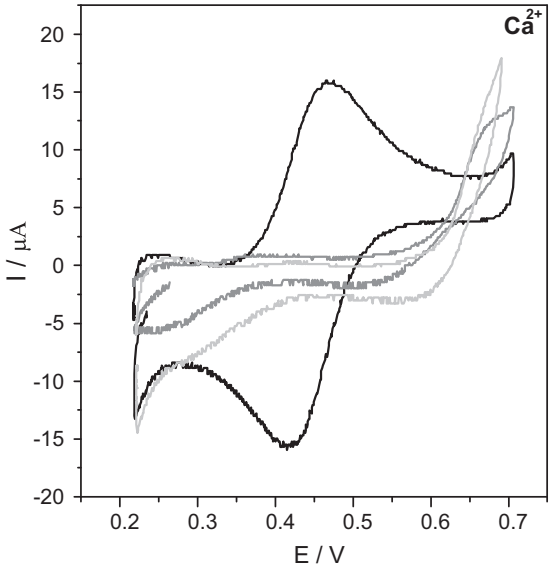

Fig. 2. Cyclic voltamograms corresponding to the transfer of TEA^+ through the bare interface (▬▬) or 60 min after the injection of 50 μL of 1 mM DSPG in 1:2 methanol:chloroform solution at different concentrations of chitosan: (▬▬) 0 and (▬▬) 1.00% (w/v). Aqueous phase composition: 1×10^{-2} M $CaCl_2$, 2.00% (v/v) acetic acid, 5×10^{-4} M TEA^+, and different concentrations of chitosan, pH 3.00. Organic phase composition: 1×10^{-2} M TPhAsDCC. $\upsilon = 0.050\ V\ s^{-1}$.

the presence of chitosan even at high concentration values. These different voltammetric responses depending on the cation present in aqueous phase can be explained taking into account that Ca^{2+} cations produce an important structuring effect on DSPG monolayers due to their strong interaction with the partially ionized anionic polar head groups of phospholipids which diminish the lateral electrostatic repulsions as it has already been reported [45]. Under these conditions, chitosan is not able of disorganizing the film, probably due to the impediment to penetrate into these very tightly compacted monolayers.

Summing up, the results obtained up here indicate that DSPG monolayer has a blocking effect on TEA^+ transfer, but its structure and permeability depend on the cation present in water, obtaining the highest ordered films in the case of Ca^{2+}. When

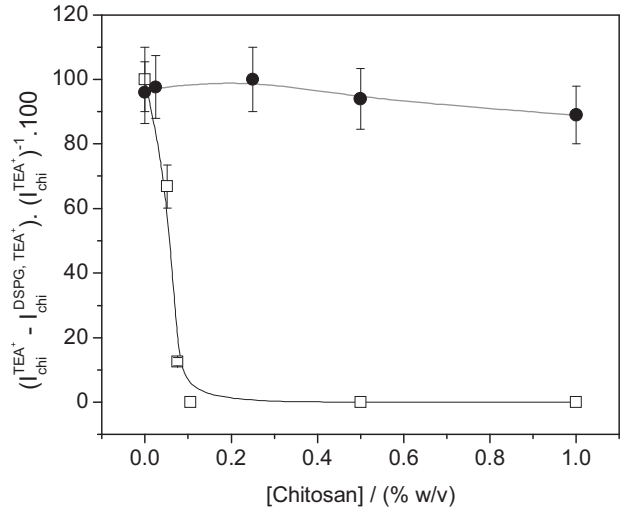

Fig. 3. Plot of blocking ratio $(I_{chi}^{TEA^+} - I_{chi}^{TEA^+,DSPG}/I_{chi}^{TEA^+} \times 100)$ vs. chitosan concentration for (□) LiCl or (●) $CaCl_2$. Organic and aqueous phase compositions are the same than in Fig. 1 (a) (□) or 2 (●).

chitosan is present in aqueous phase it is able to incorporate into DSPG monolayers formed in the presence of Li^+ producing disorganization on them, nevertheless this effect is not observed for the highly structured films formed in presence of Ca^{2+}.

3.1.2. Effect of chitosan on DSPG films previously formed

In this series of experiments the DSPG monolayer was first generated at the interface air/gelled organic phase, as described in Section 2, and subsequently this organic phase, containing the monolayer, was put in contact with the aqueous phase containing LiCl or $CaCl_2$ as supporting electrolyte in absence or in presence of chitosan. The voltammetric results (not shown) exhibited similar responses to those in Figs. 1a and 2 for LiCl and $CaCl_2$ respectively, i.e. the increasing chitosan concentration leads to increasing current values when LiCl is the aqueous electrolyte, however no changes in current values are observed in the case of $CaCl_2$.

From the comparison of the results informed in Sections 3.1.1 and 3.1.2 it can be concluded that chitosan produces disordering or pores on DSPG monolayers previously formed and also this polymer modifies the adsorption of DSPG molecules at the water/1,2-DCE interface, provided LiCl is the aqueous electrolyte.

Finally, Fig. 3 summarizes the effect of chitosan in presence of LiCl (□) or $CaCl_2$ (●). For this purpose a blocking ratio for each chitosan concentration value was calculated as:

$$\left(\frac{I_{chi}^{TEA^+} - I_{chi}^{TEA^+,DSPG}}{I_{chi}^{TEA^+}} \times 100 \right) \quad (3)$$

where $I_{chi}^{TEA^+}$ and $I_{chi}^{TEA^+,DSPG}$ are the peak current values for TEA^+ transfer process for each chitosan concentration in absence or in presence of DSPG monolayer respectively. As it can be noted, the blocking effect of the monolayer sharply decreases from 100% to values close to 0% as chitosan concentration increases in the case of LiCl, while it remains constant at values close to 100% when $CaCl_2$ is the aqueous electrolyte.

3.2. Viscosity experiments

As it was discussed above in Fig. 1b, Section 3.1.1, the transfer of TEA^+ from the aqueous to the organic phase is modified when chitosan is present in the aqueous solution even in absence of DSPG. It was noted in Fig. 1b (black triangle) that as chitosan concentration increases, the TEA^+ transfer current decreases. This behavior could be explained considering that high concentrations of chitosan produce an increase in the viscosity of the aqueous phase and, as consequence, the diffusion rate of TEA^+ from the bulk of the aqueous solution to the interface decreases. To corroborate this hypothesis, viscosity measurements were performed at $(25 \pm 1\,^{\circ}C)$ and the diffusion coefficients of TEA^+ at different chitosan concentration were calculated.

The viscosity measurements of chitosan solutions were made as described in Section 2.3. From these experiments, flow curves or rheogram, plots of shear stress (τ/Pa) vs. shear rate ($\dot{\gamma}/s^{-1}$), for different chitosan solutions were obtained and are shown in Fig. 4. As can be seen, all the solutions studied (chitosan in a concentration range from 0 to 1.00% (w/v)) present a linear flow behavior, which is characteristic of a Newtonian fluid [46], whose regimen obeys the following equation:

$$\tau = \dot{\gamma}\eta \quad (4)$$

where η is the apparent viscosity of the solution. According to this equation, the apparent viscosities for chitosan solutions were determined from the slope of the plots in Fig. 4 (Table 1). As it was expected the viscosity of chitosan solutions increase with the concentration.

On the other hand, the diffusion coefficients of TEA^+ in aqueous phase were calculated for all the chitosan solutions studied. The relation between the diffusion coefficient of TEA^+ and the peak current of transfer is given by the equation:

$$Ip^{TEA^+} = 0.4463 \cdot z \cdot F \cdot A \cdot c^{TEA^+} \cdot D_{TEA^+}^{1/2} \left(\frac{z \cdot F \cdot \nu}{R \cdot T} \right)^{1/2} \quad (5)$$

where Ip^{TEA+} is the peak current for TEA^+ transfer at each chitosan concentration; z is the charge of TEA^+; F the Faraday constant; A the interfacial area ($0.16\,cm^2$); c is the concentration of TEA^+ in aqueous phase (5.00×10^{-4} M); D is the diffusion coefficient of TEA^+, ν is the sweep rate, R the gases constant and T the temperature at witch the experiments were performed [47]. In this way, D values were calculated from the slope of Ip^{TEA+} vs. ν graphs for each chitosan concentration and, as expected, they decreased when chitosan concentration increased. From this data set, a linear relationship between the diffusion coefficient of TEA^+ (D) and the inverse of the solution viscosity (η^{-1}), with a correlation coefficient of 0.9384 and random residues, was determined (plot not shown). The linear relationship can be described in function of the Stoke–Einstein relation:

$$D = \frac{k_b.T}{f} \quad (6)$$

where k_b is the Boltzman constant; f is the frictional coefficient, a measure of the force retarding a molecule's motion. For a spherical particle of radius a in a solvent of viscosity η, the frictional coefficient is given by $f = 6\pi \cdot a \cdot \eta$ [48,49]. So that, from the slope of D vs. η^{-1}

Table 1
Values of apparent viscosity (η) for aqueous solutions with increasing chitosan concentration calculated from the slopes of plots in Fig. 5, and diffusion coefficients for TEA^+ at every chitosan concentration, obtained from voltammetric peak currents.

(Chitosan) (% w/v)	$\eta \times 10^{-4}$ (Pa s^{-1})
0	7.13
0.05	11.20
0.07	12.50
0.10	17.60
0.15	21.50
0.25	26.40
0.50	59.50
1.00	218.00

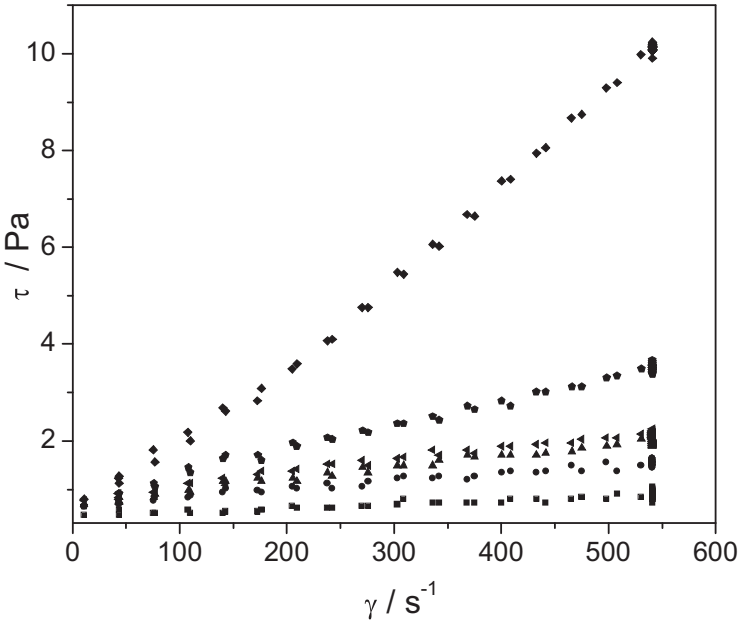

Fig. 4. Plot of shear stress (τ) as function of shear rate ($\dot{\gamma}$). Aqueous phase composition: 1×10^{-2} M LiCl, 2.00% (v/v) acetic acid and (■) 0, (●) 0.07, (▲) 0.15, (◄) 0.25, (⬟) 0.50, (⧫) 1.00% (w/v) chitosan.

plot, and assuming a spherical geometry for TEA^+, a radius $a = 3.27$ Å could be calculated, close to the value 3.4 Å, reported for TEA^+ radius in a theoretical work on the Gibbs energies of ion transfer at ITIES [50].

These results confirm that the increasing concentration of chitosan in aqueous phase produces a diminution in diffusion coefficient of TEA^+, explaining the decrease in peak currents pointed out in Section 3.1.1.

3.3. Langmuir monolayers

3.3.1. Surface pressure - molecular area isotherms

The effect of chitosan on the partially ionized anionic DSPG monolayer can be noted in Fig. 5. This figure shows the surface pressure-area isotherm obtained at 25 °C in absence and in presence of different chitosan concentrations using LiCl (Fig. 5a) and $CaCl_2$ (Fig. 5b) in the subphase. The isotherms obtained in absence of chitosan (solid line) in both media show a change in the slope characteristic to the transition gaseous-liquid condensed phase. The DSPG monolayer collapse is evident at surface pressures of 48 mN m^{-1}, with mean molecular areas of 35 Å^2 and 38 Å^2 for LiCl and $CaCl_2$ subphases respectively. Important changes in the surface pressure - area isotherms are visible when DSPG monolayer is spread on the subphases containing chitosan in both media. As it can be noted in the Fig. 5 the isotherms shift towards larger areas per molecule, indicating that chitosan was incorporated to the film at low pressures, producing an expansion of the DSPG film [25,51,52]. This expansion can also be deduced from the compression modulus values, κ (mN m^{-1}), which allow classifying the state of the monolayer as: liquid-expanded (κ =10–100 mN m^{-1}), liquid-condensed (κ =100–250 mN m^{-1}) and condense (κ > 250 mN m^{-1}) [53]. Table 2 shows the values of κ obtained at a constant pressure equal to 30 mN m^{-1} and, as it can be observed, the results indicate that in absence of chitosan the state of the monolayer corresponds to liquid-condensed phase for either, LiCl or $CaCl_2$ subphases. Nevertheless, as chitosan concentration increases, the modulus κ decreases reaching values of 20–30 mN m^{-1} for the highest chitosan concentration employed. This observation indicates the presence of a new component at the interface, which

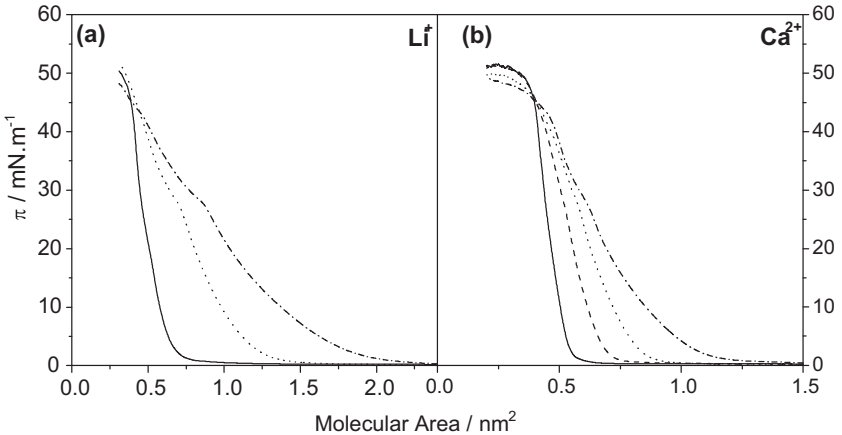

Fig. 5. Surface pressure (π) as function of the mean molecular area for DSPG monolayer at the air–water interface. Subphase composition: 2.00% (v/v) acetic acid, chitosan: (a) (▬▬) 0, (…) 0.02 and (-..-) 0.06% (w/v) in 1×10^{-2} M LiCl (b) (▬▬) 0, (-..-) 0.01, (…) 0.02 and (-..-) 0.06% (w/v) in 1×10^{-2} M $CaCl_2$. pH 3.00.

Table 2
Compression modulus, κ, for DSPG monolayer formed on subphases containing 1×10^{-2} M LiCl or 1×10^{-2} M $CaCl_2$ in absence or in presence of different chitosan concentrations. The values of κ were calculated at $\pi = 30\,mN\,m^{-1}$.

(Chitosan)/(% w/v)	κ/mN m^{-1}	
	LiCl	$CaCl_2$
0	104	125
0.01	55	68
0.02	27	48
0.06	22	31

produces changes in the state of the monolayer from liquid-condense to liquid-expanded phase. The great change of the compression modulus at high surface pressures was attributed, by Pavinatto et al., to the interaction between chitosan and the phospholipid polar head group which makes the film more flexible [52]. This effect can be clearly observed in Fig. 6a where the change in the area per molecule ($\Delta A = A^{\text{in presence of chitosan}} - A^{\text{in absence of chitosan}}$), produced by chitosan, at 25 mN m^{-1} and 40 mN m^{-1} are shown. As can be noted, the increase in area is more pronounced at low pressure, condition at which the incorporation of chitosan into the film is more feasible. As the monolayer is compressed (pressure 40 mN m^{-1}), lower values of ΔA are obtained, as a consequence of the expelling of a certain amount of chitosan from the surface. On the other hand, comparing ΔA values for subphases containing LiCl or $CaCl_2$, it is evident that in the first case the shift of the isotherm, towards higher A values, is more important. An explanation for this behavior can be found in the higher charge density of Ca^{2+} compared with Li^+, which leads to a higher accumulation of this cation at the surface where the negative charge of polar head groups of DSPG are located, and, additionally, to a direct binding to the phosphate groups of DSPG. The strong interaction Ca^{2+} – phosphate results in the reduction of the electrostatic repulsion between the polar head groups and an enhancement of the interaction between the hydrocarbon tails of DSPG leading to a greater structuring of the monolayer. The effect on monolayer condensation produced by different cations has been also shown by means of electrochemical experiments for various phospholipid [37,38]. Based on these reports and considering the results shown in Fig. 6, it can be stated that chitosan may be incorporated in the monolayer in a more effective way when LiCl is present in the subphase instead of $CaCl_2$, producing an important change in the resulting average molecular area.

The effect of expansion of the DSPG film produced by chitosan is also evident when the pressure and the molecular area in the collapse, as a function of chitosan concentration, are analyzed. Fig. 6b shows this variation for subphases containing LiCl (circles) or $CaCl_2$ (squares). For both cases an enhancement of the collapse molecular area with the increasing chitosan concentration was observed. This result demonstrates that chitosan is not completely expelled from the interface when the monolayer arrive to the collapse, at this point chitosan remains in the interface interacting with the partially ionized negative polar head groups of DSPG. It can also be observed in Fig. 6b that DSPG monolayers in the presence of chitosan collapse at surface pressures lower than those of pure DSPG, thus indicating that they are less resistant to compression than the pure monolayer.

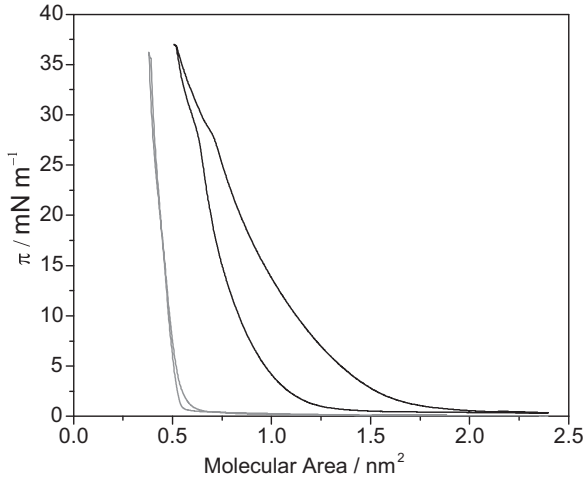

Fig. 7. Surface pressure (π) as a function of the mean molecular area for one cycle of compression–decompression of DSPG monolayer for subphases containing: 1×10^{-2} M LiCl and ( ) 0 or ( ) 0.06% (w/v) chitosan.

Furthermore, compression-decompression curves has been carried out for pure DSPG and mixed chitosan-DSPG monolayers, Fig. 7. For pure DPPG monolayer no hysteresis is observed (grey line) in the isotherm. On the opposite, for chitosan-DSPG monolayers a significant hysteresis is observed (black line), probably due to the formation of an irreversible complex between DSPG and chitosan which can aggregate at the interface. This effect has been previously reported by Pavinatto et al. for DPPG and DPPC monolayers in the presence of chitosan [52].

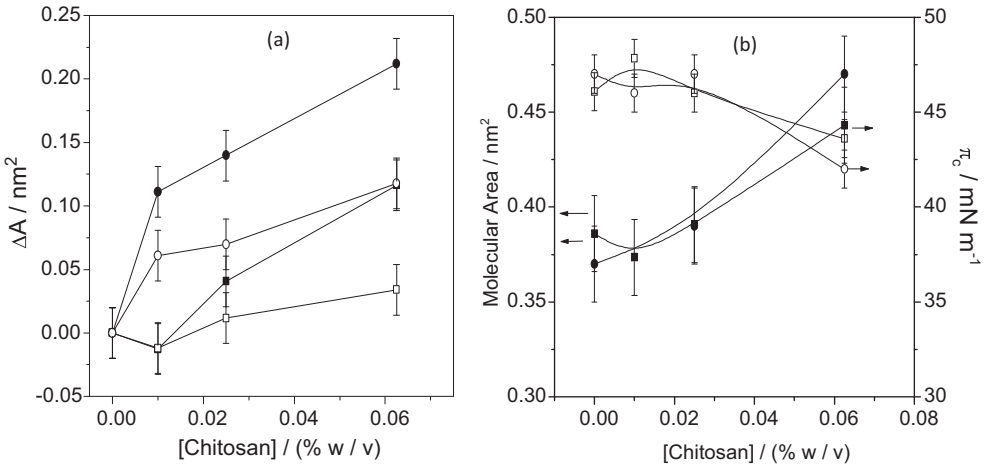

Fig. 6. (a) Change in area per molecule at (■, ●) 25 mN m^{-1} and (□, ○) 40 mN m^{-1} for a Langmuir film of DSPG as function of chitosan concentration. (b) Collapse pressure (□, ○) and collapse area (■, ●) vs. chitosan concentration. Subphase composition: 2.00% (v/v) acetic acid and (●, ○) 1×10^{-2} M LiCl or (■, □) 1×10^{-2} M $CaCl_2$ and different chitosan concentrations. pH 3.00.

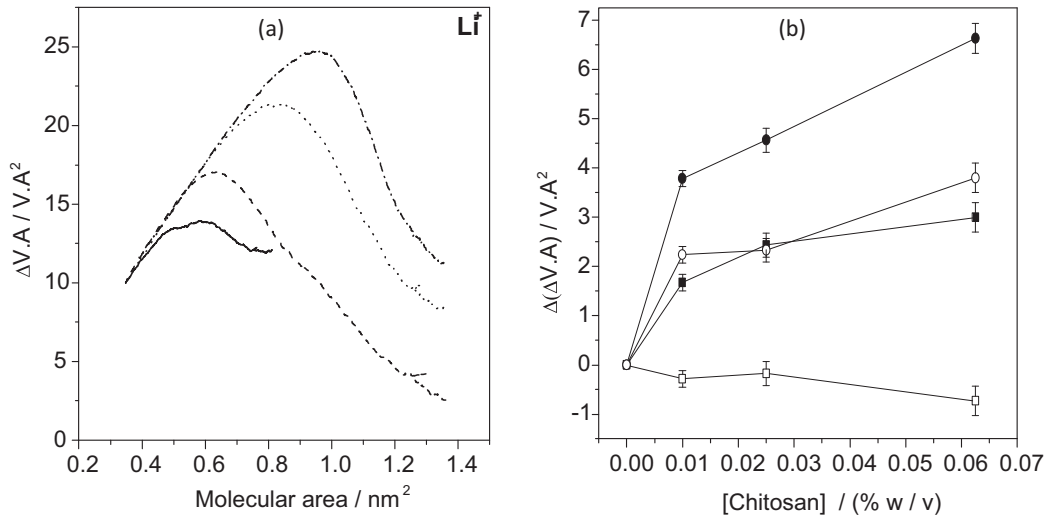

Fig. 8. (a) Isotherms of surface potential per area per molecule ($\Delta V{\cdot}A$) for subphases containing: 1×10^{-2} M LiCl, 2.00% (v/v) acetic acid in absence (▬) and in presence of chitosan (--) 0.01, (···) 0.02 and (-·-) 0.06% (w/v). (b) Variation of $\Delta(\Delta V{\cdot}A)$ (see text) with chitosan concentration at different pressures: (■, ●) 25 mN/m and (□, ○) 40 mN/m for subphases containing (●, ○) 1×10^{-2} M LiCl or (■, □) 1×10^{-2} M $CaCl_2$.

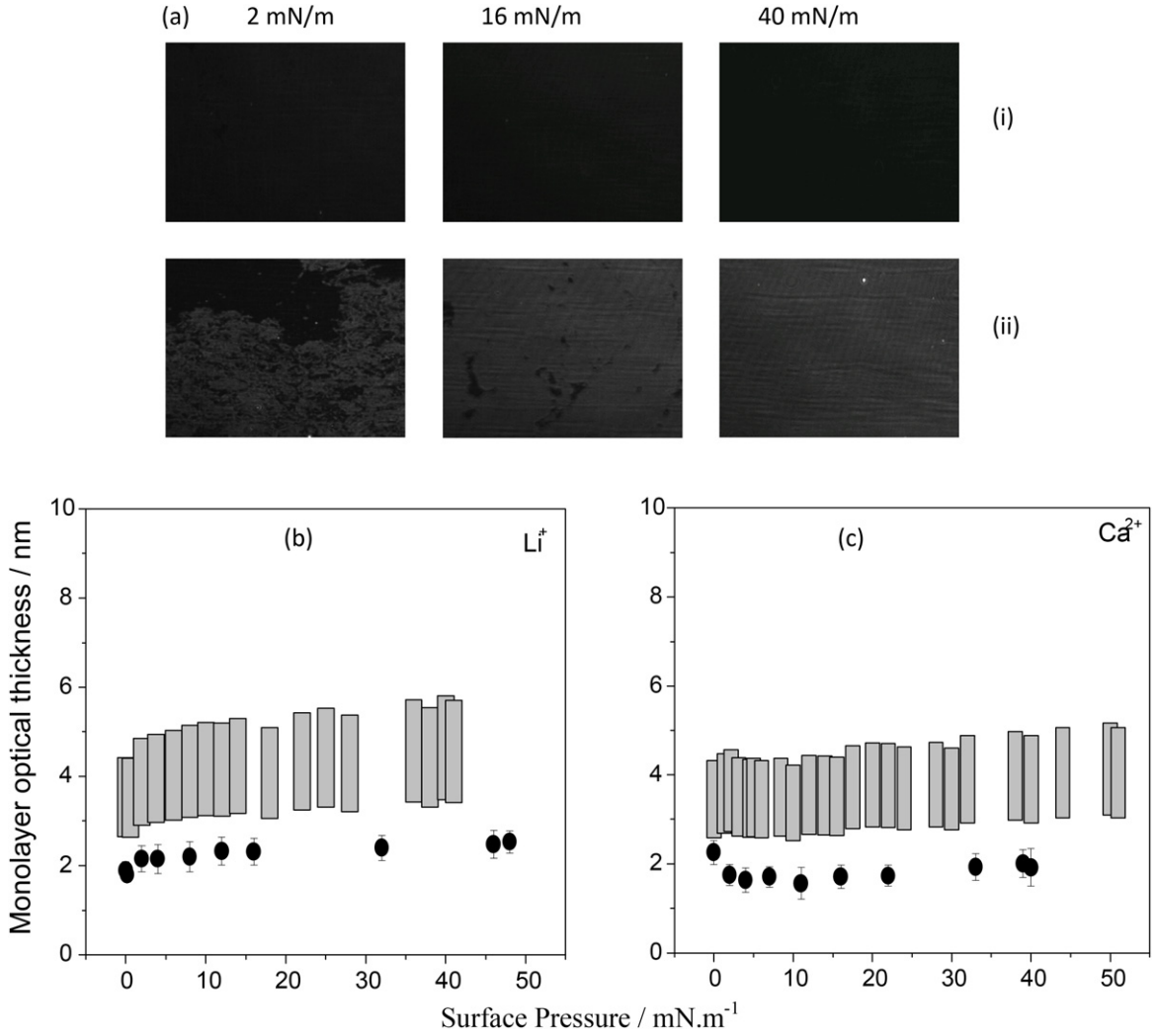

Fig. 9. (a) BAM images for monolayers of DSPG in 1×10^{-2} M $CaCl_2$, 2,00% (v/v) acetic acid, without (i) and with (ii) 0.06% (w/v) chitosan. (b) and (c) Monolayer optical thickness for subphases containing 2.00% (v/v) acetic acid and (a) 1×10^{-2} M LiCl or (b) 1×10^{-2} M $CaCl_2$ in absence (●) and in presence (▩) of chitosan (whole range of possible values).

3.3.2. Surface potential - area isotherms

Fig. 8a shows the change of surface potential per molecular area ($\Delta V{\cdot}A$, which is proportional to the apparent dipole moment of the monolayer) as function of the mean molecular area, for DSPG monolayer at different chitosan concentration in the subphase. As the monolayer is compressed, $\Delta V{\cdot}A$ increases as a consequence of the orientation of polar head groups, the hydrocarbon chains or the hydration water at the interface as well as of changes in the double-layer contribution. When chitosan is present, an excess of positive charge is present at the interface interacting with the polar head groups of DSPG generating an alteration of the average vertical component of the dipole moment of DSPG molecules and producing an enhancement of $\Delta V{\cdot}A$. Another explanation for this increase in potential can be found in the reorganization of the dipolar moment of the interfacial molecules of water around chitosan [26]. Similar effect was observed when the subphase contained $CaCl_2$ as electrolyte (data not shown).

Fig. 8b shows the change of surface potential per unit of area produced by different chitosan concentrations, calculated as: $(\Delta(\Delta V \cdot A)) = (\Delta V \cdot A_{\text{with chit}} - \Delta V \cdot A_{\text{without chit}})$ at two lateral pressures (25 and 40 mN m^{-1}), as a function of the chitosan concentration in subphases containing LiCl (circles) or $CaCl_2$ (squares). As can be observed, the increase of surface potential is evident for LiCl subphases both at low (25 mN m^{-1}) and high pressures (40 mN m^{-1}), indicating that chitosan prevails interacting with the phospholipid and is not expelled from the interface to the bulk subphase, even at pressures near to the collapse. Nevertheless, chitosan generates higher increases of the surface potential when the film is at low pressure, corresponding with the fact that chitosan can penetrate more efficiently in the DSPG film contributing with its positive charge. When the subphase contains $CaCl_2$ almost constant Δ ($\Delta V{\cdot}A$) values are observed over the whole range of chitosan concentrations at high pressure, while comparing the response obtained for LiCl and $CaCl_2$ at low pressure, it is evident that the increase in Δ ($\Delta V{\cdot}A$) is more pronounced when LiCl is present in the subphase. This is in agreement with the fact that the films generated in presence of LiCl are less condensed that those formed in presence of $CaCl_2$, as discussed above in Section 3.3.1, allowing a better incorporation of chitosan into the DSPG monolayer.

3.4. Brewster angle microscopy (BAM)

Brewster angle microscopy studies were performed with the aim of confirming the presence of chitosan at the interface interacting with the DSPG monolayer. Fig. 9a shows representative micrographs obtained by BAM, for the DSPG film in absence (i) and in the presence (ii) of 0.06% w/v solution of chitosan in 1×10^{-2} M $CaCl_2$ and 2.00% (v/v) acetic acid, at different lateral pressures. As it can be observed, there is a noticeable difference between the gray levels of the micrograph for DSPG films and mixed DSPG–chitosan films. As stated in the previous sections, we attribute these differences to the fact that chitosan interacts with DSPG molecules, both at low and high pressures, generating an enhancement in the surface thickness. The difference in gray levels was also observed using LiCl as aqueous electrolyte (micrograph not shown).

With the purpose of showing the results in a more quantitative manner, the optical thickness of the monolayer was calculated using the Eq. (2). The refractive index used for DSPG monolayers in the absence of chitosan was 1.45, since this is the value reported for condensed films [44]. When chitosan is present in the subphase the DSPG film becomes less dense and then, the refractive index is expected to decrease [44]. Since the refractive index at this condition was unknown, we determined the optical thicknesses of the monolayer using 1.42 (refractive index for a liquid expanded phases) or 1.45 [43] (refractive index for a liquid condensed phases)

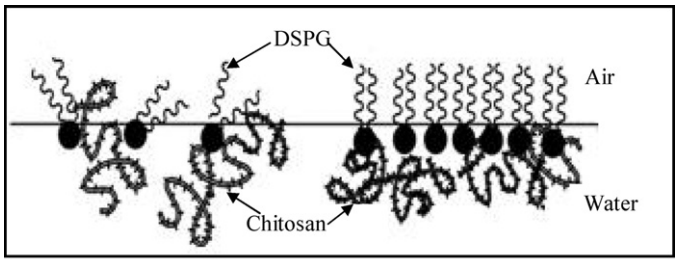

Scheme 2. Schematic model for DSPG–chitosan interaction at the air/water interface for (a) high or (b) low molecular areas.

and the whole range of possible optical thicknesses values as function of surface pressure were plotted in Fig. 9b and c in comparison with values obtained in absence of chitosan.

For both electrolytes (LiCl or $CaCl_2$) the monolayer thickness in absence of chitosan was around 20 Å. When chitosan is present in the subphase, the thickness values are in the range between 30 and 50 Å, overcoming the values obtained for pure DSPG monolayer for all the pressure measured. These results are another evidence that chitosan is present at the interface, interacting with DSPG molecules, even at high lateral pressure values.

4. Conclusions

Taking into account the results obtained in the present paper, we propose the model shown in Scheme 2 for the interaction between DSPG and chitosan. In this model two stages for the interaction of chitosan with DSPG can be distinguish: in first place, at low pressures (large molecular areas), the interaction is driven by Van der Waals forces between the DSPG hydrocarbon tails and the hydrophobic zones of chitosan. This interaction is facilitated by chitosan penetration into the monolayer in gaseous state. Beside the hydrophobic interaction, electrostatic attraction between the phosphate groups of DSPG and the positive charged amino groups of chitosan can also be established (Scheme 2a).

Secondly, at high pressures, chitosan is partially expelled from the interface, but it remains at the interface interacting with DSPG monolayer probably through electrostatic interaction between phosphate and the amino groups.

The situation at liquid/liquid interfaces with LiCl as aqueous electrolyte is, probably, similar to that shown in Scheme 2a, obtaining a blocking film in absence of chitosan and a more permeable one in presence of the polymer, explaining in this way the electrochemical results. On the other hand, the presence of $CaCl_2$ as supporting aqueous electrolyte produces more compact monolayers, similar to that shown in Scheme 2b, which can not be penetrated by chitosan molecules prevailing the blocking effect of DSPG film to TEA^+ transfer.

Acknowledgements

Financial support from Consejo Nacional de Investigaciones Científicas y Tecnológicas (CONICET), Agencia Nacional de Promoción Científica y Tecnológica (FONCyT) and Secretaría de Ciencia y Técnica de la Universidad Nacional de Córdoba (SECyT) is gratefully acknowledged. C.I. Cámara and M.V. Colqui Quiroga wish to thank CONICET for the fellowships awared. A. Jimenez-Kairuz, N. Wilke and L.M. Yudi are members of the Research Career of CONICET.

References

[1] W. Sui, G. Song, G. Chen, G. Xu, Aggregate formation and surface activity property of an amphiphilic derivative of chitosan, Colloids and Surfaces A: Physicochemical and Engineering Aspects 256 (2005) 29.

[2] M. Rinaudo, Chitin and chitosan: properties and applications, Progress in Polymer Science 31 (2006) 603.
[3] R.N. Tharanathan, F.S. Kittur, Chitin – the undisputed biomolecule of great potential, Critical Reviews in Food Science and Nutrition 43 (2003) 61.
[4] M.N.V. Ravi Kumar, A review of chitin and chitosan applications, Reactive and Functional Polymers 46 (2000) 1.
[5] M. Yalpani, F. Johnson, L.E. Robinson, Chitin, Chitosan: Sources, Chemistry, Biochemistry, Physical Properties and Application, Elsevier, Amsterdam, 1992.
[6] S.F. Ausar, I.D. Bianco, R.G. Badini, L.F. Castagna, N.N. Modesti, C.A. Landa, D.M. Beltramo, Characterization of casein micelle precipitation by chitosans, Journal of Dairy Science 84 (2001) 361.
[7] F.C. Wu, R.L. Tseng, R.S.J. Juang, A review and experimental verification of using chitosan and its derivatives as adsorbents for selected heavy metals, Environmental Management 91 (2010) 798.
[8] B. Krajawska, Membrane-based processes performed with use of chitin/chitosan materials, Separation and Purification Technology 41 (2005) 305.
[9] K.M. Shields, N. Smock, C.E. McQueen, P.J. Bryant, Chitosan for weight loss and cholesterol management, American Journal of Health-System Pharmacy 60 (2003) 1310.
[10] J. Sun, G. Jiang, Y. Wang, F.J. Ding, Thermosensitive chitosan hydrogel for implantable drug delivery: blending PVA to mitigate body response and promote bioavailability, Applied Polymer Science 125 (2012) 2092.
[11] J. Yun-Huan, H. Hai-Yang, Q. Ming-Xi, Z. Jia, Q. Jia-Wei, H. Chan-Juan, Z. Qiang, C. Da-Wei, pH-sensitive chitosan-derived nanoparticles as doxorubicin carriers for effective anti-tumor activity: preparation and in vitro evaluation, Colloid and Surfaces B: Biointerface 94 (2012) 184.
[12] H.S. Moussa, A.A. Tayel, A.I. Al-Turki, Evaluation of fungal chitosan as a biocontrol and antibacterial agent using fluorescence-labeling, International Journal of Biological Macromolecules 54 (2013) 204.
[13] F. Shahidi, J.K. Vidana Arachchi, Y.J. Jean, Food applications of chitin and chitosans, Trends in Food Science & Technology 10 (1999) 37.
[14] Y. Okamoto, R. Yano, K. Miyatake, I. Tomohiro, Y. Shigemasa, S. Minami, Effects of chitin and chitosan on blood coagulation, Carbohydrate Polymers 53 (2003) 337.
[15] N. Fang, V. Chan, Interaction of liposome with immobilized chitosan during main phase transition, Biomacromolecules 4 (2003) 581.
[16] L. Caseli, F.J. Pavinatto, T.M. Nobre, M.E.D. Zaniquelli, T. Viitala, O.N. Oliveira Jr., Chitosan as a removing agent of β-lactoglobulin from membrane models, Langmuir 24 (2008) 4150.
[17] C.A. Silva, T.M. Nobre, F.J. Pavinatto, O.N. Oliveira Jr., Interaction of chitosan and mucin in a biomembrane model environment, Journal of Colloids and Interface Science 376 (2012) 289.
[18] J.M. Campiña, H.K.S. Souza, J. Borges, A. Martins, M.P. Gonçalves, F. Silva, Studies on the interactions between bovine β-lactoglobulin and chitosan at the solid–liquid interface, Electrochimica Acta 55 (2010) 8779.
[19] B. Krajewska, P. Wydro, A. Janczyk, Probing the modes of antibacterial activity of chitosan. Effects of pH and molecular weight on chitosan interactions with membrane lipids in Langmuir films, Biomacromolecules 12 (2011) 4144.
[20] F.J. Pavinatto, C.P. Pacholatti, E.A. Montanha, L. Casei, H.S. Silva, P.B.T. Miranda, O.N. Oliveira Jr., Cholesterol mediates chitosan activity on phospholipid monolayers and Langmuir–Blodgett films, Langmuir 25 (2009) 10051.
[21] N. Fang, V. Chan, Chitosan-induced restructuration of a mica-supported phospholipid bilayer: an atomic force microscopy study, Biomacromolecules 4 (2003) 1596.
[22] F. Yang, X. Cui Yang Xiurong, Interaction of low-molecular-weight chitosan with mimic membrane studied by electrochemical methods and surface plasmon resonance, Biophysical Chemistry 99 (2002) 99.
[23] V. Chan, H.Q. Mao, K.W. Leong, Chitosan-induced perturbation of dipalmitoyl-sn-glycero-3-phosphocholine membrane bilayer, Langmuir 17 (2001) 3749.
[24] N. Fangi, V. Chan, H.Q. Mao, K.W. Leong, Interactions of phospholipid bilayer with chitosan: effect of molecular weight and pH, Biomacromolecules 2 (2001) 1161.
[25] H. Parra-Barraza, M.G. Burboa, M. Sánchez-Vazquez, J. Juárez, F.M.G. Goycoolea, M.A. Valdez, Chitosan–cholesterol and chitosan–stearic acid interactions at the air–water interface, Biomacromolecules 6 (2005) 2416.
[26] F.J. Pavinatto, L. Casei, A. Pavinatto, D.S. dos Santos Jr., T.M. Nobre, M.E.D. Zaniquelli, H.S. Silva, P.B.T. Miranda, O.N. Oliveira Jr., Probing chitosan and phospholipid interactions using Langmuir and Langmuir–Blodgett films as cell membrane models, Langmuir 23 (2007) 7666.
[27] T. Kakiuchi, Y. Teranishi, K. Niki, Adsorption of sorbitan fatty acid esters and a sucrose mono-alkanoate at the nitrobenzene-water interface and its effect on the rate of ion transfer across the interface, Electrochimica Acta 40 (1995) 2869.
[28] H. Jänchenová, K. Stulik, V.J. Marecek, Adsorption and ion-pairing interactions of phospholipids in the system of two immiscible electrolyte solutions Part I. The behaviour of lecithin at the water/1,2-dichloroethane interface, compared with that of trimethyloctadecylammonium cation, Journal of Electroanalytical Chemistry 601 (2007) 101.
[29] S.O'. Sullivan, D.M.W. Arrigan, Electrochemical behaviour of myoglobin at an array of microscopic liquid–liquid interfaces, Electrochimica Acta 77 (2012) 71.
[30] G. Herzog, V. Kam, D.M.W. Arrigan, Electrochemical behaviour of haemoglobin at the liquid/liquid interface, Electrochimica Acta 53 (2008) 7204.
[31] A. Berduque, M.D. Scanlon, C.J. Collins, D.W.M. Arrigan, Electrochemistry of non-redox-active poly(propylenimine) and poly(amidoamine) dendrimers at liquid–liquid interfaces, Langmuir 23 (2007) 7356.
[32] S.G. Chesniuk, S.A. Dassie, L.M. Yudi, A.M. Baruzzi, Electrochemical study of the interaction of alkali and alkaline-earth cations with a dibehenoyl phosphatidylcholine monolayer at the water/1,2-dichloroethane interface, Electrochimica Acta 43 (1998) 2175.
[33] M.A. Mendez, M. Prudent, B. Su, H.H. Girault, Peptide–phospholipid complex formation at liquid–liquid interfaces, Analytical Chemistry 80 (2008) 9499.
[34] J.S. Riva, K. Bierbrauer, D.M. Beltramo, L.M. Yudi, Electrochemical study of the interfacial behavior of cationic polyelectrolytes and their complexation with monovalent anionic surfactants, Electrochimica Acta 85 (2012) 659.
[35] J.S. Riva, A.V. Juarez, D.M. Beltramo, L.M. Yudi, Interaction of Chitosan with mono and di-valent anions in aqueous solution studied by cyclic voltammetry at a water/1,2-dichloroethane interface, Electrochimica Acta 59 (2012) 39.
[36] G. Herzog, D.M.W. Arrigan, Interaction of acridine-calix[4]arene with DNA at the electrified liquid|liquid interface, Electrochimica Acta 55 (2010) 3348.
[37] L.M.A. Monzón, L.M. Yudi, Electrochemical study of flunitrazepam partitioning into zwitterionic phospholipid monolayers, Electrochimica Acta 51 (2006) 1932.
[38] L.M.A. Monzón, L.M. Yudi, Flunitrazepam effect on distearoylphosphatidylglycerol, cholesterol and distearoylphosphatidylglycerol + cholesterol mixed monolayers structure at a DCE/water interface, Electrochimica Acta 51 (2006) 4573.
[39] L.M.A. Monzón, L.M. Yudi, Cation adsorption at a distearoylphosphatidic acid layer adsorbed at a liquid/liquid interface, Electrochimica Acta 52 (2007) 6873.
[40] M.V. Colqui Quiroga, L.M.A. Monzón, L.M. Yudi, Voltammetric study and surface pressure isotherms describing Flunitrazepam incorporation into a distearoylphosphatidic acid film adsorbed at air/water and water/1,2-dichloroethane interfaces, Electrochimica Acta 56 (2011) 7022.
[41] M.V. Colqui Quiroga, L.M.A. Monzón, L.M. Yudi, Interaction of triflupromazine with distearoylphosphatidylglycerol films studied by surface pressure isotherms and cyclic voltammetry at a 1,2-dichloroethane/water interface, Electrochimica Acta 55 (2010) 5840.
[42] F. Vega Mercado, B. Maggio, N. Wilke, Phase diagram of mixed monolayers of stearic acid and dimyristoylphosphatidylcholine. Effect of the acid ionization, Chemistry and Physics of Lipids 164 (2011) 386.
[43] J.G. Petrov, T. Pfohl, H. Mohwald, Ellipsometric chain length dependence of fatty acid Langmuir monolayers. A Heads-and-Tails model, Journal of Physical Chemistry B 103 (1999) 3417.
[44] D. Ducharme, J.J. Max, C. Salesse, R.M. Leblanc, Ellipsometric study of the physical states of phosphatidylcholines at the air–water interface, Journal of Physical Chemistry 94 (1990) 1925.
[45] P. Garidel, A. Blume, 1,2-Dimyristoyl-sn-glycero-3-phosphoglycerol (DMPG) monolayers: influence of temperature, pH, ionic strength and binding of alkaline earth cations, Chemistry and Physics of Lipids 138 (2005) 50.
[46] J. Desbrieres, Viscosity of semiflexible chitosan solutions: influence of concentration, temperature, and role of intermolecular interactions, Biomacromolecules 3 (2002) 342.
[47] A.J. Bard, L.R. Faulkner, Electrochemical Methods, Fundamentals and Applications, 2nd ed., John Wiley and Sons Inc., New York, 2000.
[48] P. Atkins, J. de Paula, Physical Chemistry, 7th ed., Oxford University Press, New York, 2006.
[49] R. Srivastava, K.N. Khanna, Stokes–Einstein relation in two- and three-dimensional fluids, Journal of Chemical and Engineering Data 54 (2009) 1452.
[50] R.A.W. Dryfe, S.M. Holmes, Zeolitic rectification of electrochemical ion transfer, Journal of Electroanalytical Chemistry 483 (2000) 144.
[51] P. Wydro, B. Krajewska, H.W. Katarazyna, Chitosan as a lipid binder: a Langmuir monolayer study of chitosan–lipid interactions, Biomacromolecules 8 (2007) 2611.
[52] F.J. Pavinatto, A. Pavinatto, L. Casei, L.D.S. dos Santos Jr., T.M. Nobre, M.E.D. Zaniquelli, O.N. Oliveira Jr., Interaction of chitosan with cell membrane models at the air–water interface, Biomacromolecules 8 (2007) 1633.
[53] J.T. Davies, E.K. Rideal, Interfacial Phenomena, Academic Press, New York, 1963.